Publisher: GSA
Journal: GEOL: Geology
Article ID: G25284

Deposition of highly crystalline graphite from moderate-temperature fluids

F.J. Luque[1*], L. Ortega[1], J.F. Barrenechea[1], D. Millward[2], O. Beyssac[3], J-M. Huizenga[4]

[1]*Departamento de Cristalografía y Mineralogía, Facultad de Geología, Universidad Complutense de Madrid, 28040 Madrid, Spain*

[2]*British Geological Survey, Murchison House, West Mains Road, Edinburgh EH9 3LA, UK*

[3]*Laboratoire de Géologie, CNRS, Ecole Normale Supérieure, 24 rue Lhomond, 75005 Paris, France*

[4]*Department of Geology, University of Johannesburg, P.O. Box 524, Auckland Park 2006, University & Kingsway (APK campus), Johannesburg, South Africa*

*E-mail: jluque@geo.ucm.es

ABSTRACT

Recognized large occurrences of fluid-deposited graphite displaying high crystallinity are so far restricted to high-temperature environments (mainly granulite facies terranes). However, in the extensively mined Borrowdale deposit (UK), the mineralogical assemblage, notably the graphite-epidote intergrowths, shows that fully-ordered graphite precipitated during the propylitic hydrothermal alteration of the volcanic host rocks. Fluids responsible for graphite deposition had an average XCO_2/XCO_2+XCH_4 ratio of 0.69, thus indicating temperatures of ~500 ºC at the FMQ buffered conditions.

Publisher: GSA
Journal: GEOL: Geology
Article ID: G25284

Therefore, this is the first reported evidence indicating that huge concentrations of highly crystalline graphite can precipitate from moderate-temperature fluids.

INTRODUCTION

The progressive transformation of carbonaceous matter through prograde metamorphism (graphitization) and the deposition from C-O-H fluids are the two major processes responsible for the formation of graphite in rocks. Transformations induced by metamorphism of carbonaceous matter include both structural and chemical modifications that eventually lead to the formation of graphite. Thus, metamorphic graphite distinctively shows a wide range of structural ordering that can be correlated with metamorphic grade, mainly with temperature (Landis, 1971; Wopenka and Pasteris, 1993; Wada et al., 1994; Nishimura et al., 2000; Beyssac et al., 2002). That is, "crystallinity", described as the degree of crystalline perfection (i.e., the similarity of a given arrangement of carbon atoms to the ideal graphite structure, both along the stacking direction of the carbon layers and along the a-b plane), increases with metamorphic grade. Compared with metamorphic graphite, fluid-deposited graphite in volumetrically large occurrences is known at the present to be restricted to high-temperature environments and universally displays high crystallinity (Luque et al., 1998; Luque and Rodas, 1999; Pasteris, 1999). Small-volume, poorly crystalline fluid-deposited graphite has been described associated with hydrothermal gold-quartz veins (Mastalerz et al., 1995) or along shear zones (Pasteris and Chou, 1998). Precipitation of graphite has also been observed within fluid inclusions, both by natural and experimental mechanisms involving re-equilibration of metastable C-O-H fluids (Cesare, 1995; Satish-Kumar,

2005; and references therein). Such mechanisms systematically resulted in the formation of poorly crystalline graphite.

This paper presents the first known evidence from a large graphite deposit of highly crystalline graphite precipitated from moderate-temperature fluids. This evidence comes from the mineral assemblages and textural relationships between graphite and other mineral phases, along with fluid inclusion microthermometric data from the historic Borrowdale graphite deposit in NW England (UK). The findings of this study clearly contrast with previous work that argued against volumetrically large highly-crystalline graphite deposits being precipitated from carbon-bearing fluids at low-pressures and low to moderate temperatures (Pasteris, 1999). In addition, this study sheds new light on the constraints controlling highly crystalline graphite precipitation from low- to moderate-temperature fluids, which could be of interest for laboratory, and even industrial, synthesis.

GEOLOGICAL AND PETROGRAPHICAL CHARACTERISTICS OF THE DEPOSIT

The Borrowdale graphite deposit consists of mineralized faults hosted by andesite lavas and sills belonging to the upper Ordovician (Caradoc) Borrowdale Volcanic Group, and by a probably contemporaneous hypabyssal dioritic intrusion (Millward, 2004). This epigenetic deposit is unique worldwide since it is the only economic concentration of graphite hosted by volcanic rocks. Mining at Seathwaite began, at least, as early as in the late 16th century, and continued until the late 19th century, producing material for the casting of cannonballs and as the basis for the renowned Keswick pencil industry.

Publisher: GSA
Journal: GEOL: Geology
Article ID: G25284

The graphite mineralization occupies about a 400 m length of a conjugate set of normal faults hading up to 45°. Strens (1965) recorded five faults striking 158–182° and three at 105°. Narrow veins and stringers filling the faults comprise massive graphite and chlorite along with quartz, but the richest deposits are developed at the intersections of the faults where there are steeply inclined pipe-like bodies up to 1 × 3 m in cross-section and from a few meters to over 100 m in length (Ward, 1876). The pipe-like bodies contain nodular masses and patches of graphite, typically 1–2 cm across, but ranging from a few millimeters to 1 m or more; the yellow-brown matrix comprises intensely altered wall-rock and brecciated quartz.

Graphite crystals in the nodules and patches from the pipes display three different morphologies: flakes (the most abundant morphology in the deposit, >90%), cryptocrystalline graphite (mostly as colloform masses usually surrounded by flaky graphite), and spherulites (5–40 μm in diameter, within laminar graphite). Graphite nodules and patches frequently include radiating aggregates of elongate epidote crystals, chlorite, polycrystalline quartz, pyrite, chalcopyrite and minor sericite. In particular, epidote is restricted to nodules composed exclusively of flaky graphite.

The andesite and dioritic wall rocks adjacent to the veins have been intensely hydrothermally altered to an assemblage containing quartz, chlorite, and albite, along with some disseminated small aggregates of graphite and late calcite veinlets. These features are indicative of an intense propylitic alteration, and evidence that graphite precipitated during this hydrothermal event.

FLUID INCLUSION DATA

A study of fluid inclusions in quartz fragments from the pipes has allowed characterization of the fluid responsible for graphite deposition. The quartz fragments contain abundant two-phase vapor-rich inclusions, made up of a mixture of H_2O, CO_2 and CH_4. These are secondary inclusions along trails within the clear cores of the quartz grains, representing the earliest fluids circulating during brecciation of the quartz and transport of the fragments upwards within the breccia pipes. This transport was coeval with major graphite precipitation along these structures, as evidenced from the textural relationships between graphite and quartz fragments in the pipes. These inclusions likely represent the composition of the fluid just before graphite saturation was reached. Microthermometric and Raman data from this fluid inclusion assemblage indicate an average fluid bulk composition (mol fraction) of 0.65 H_2O, 0.24 CO_2, 0.11 CH_4 and 1.4 wt% NaCl, a $XCO_2/(XCO_2+XCH_4)$ ratio of 0.69, a total carbon concentration in the fluid of 11 % atomic C and an average molar volume of 40 $cm^3.mol^{-1}$. Calculations were performed with the computer program *DENSITY* version 12/02 (Bakker, 1997; Bakker and Brown, 2003) using the Duan et al. (1992a, b) equation of state. Total homogenization of the inclusions in the ranges 295–340 ºC (V) and 328–350 ºC (C) indicate a minimum temperature of fluid circulation of 350 ºC.

Actual temperatures of graphite precipitation from this fluid can be estimated from the fluid composition and the oxidation state of the system at that moment. The intergrowth of flaky graphite and epidote indicates that the minerals are coeval. Epidote is not stable for $XCO_2>0.2$ (Liou, 1993). Textural relationships suggest that flaky graphite (in which epidote occurs) precipitated after spherulitic and cryptocrystalline graphite. The only way that the CO_2 content (and indeed the bulk carbon content) of the

fluid would decrease (and stabilize epidote) is if through cooling, the graphite field continued to enlarge and thereby lower the concentration of carbon in the co-existing fluid. Thus, it is likely that epidote crystallization was triggered by CO_2 depletion in the fluid caused by the early graphite precipitation (spherulites and colloform aggregates) which, in turn, would be related to hydration reactions occurring during the simultaneous propylitic alteration of the host rock. Precipitation of hydrous minerals (mainly chlorite) in the propylitic assemblage would depleted the fluid in H_2O, thereby enriching the remaining fluid in C and driving it to graphite saturation (Duke and Rumble, 1986; Luque et al., 1998). On the other hand, it is well known that the Fe^{3+} content in epidote is extremely dependent upon fO_2 (Liou, 1993). Within the graphite nodules, the composition of the epidote is Ps_{25}, expressed as the pistacite proportion, indicating an oxygen fugacity buffered at the FMQ (Liou, 1993). Thermodynamic calculations show that carbon-saturated fluids with a gas $XCO_2/(XCO_2+XCH_4)$ of 0.69 and an fO_2 in equilibrium with the FMQ buffer, are stable at temperatures of ~490 °C. Calculations were carried out using thermodynamic data for fluid species and graphite from Holland and Powell (1998). Fugacity coefficients were calculated using the equations of state after Shi and Saxena (1992). The FMQ buffer from Ohmoto and Kerrick (1977) was used. These calculations were done for a pressure of 2–3 kbar, compatible with pressure estimates inferred from emplacement of the graphite deposit in a subvolcanic setting (Millward, 2004). A pressure below 2 kbar is not possible as graphite is not stable under these conditions for the given fluid composition (Frost, 1979). A deviation from FMQ of plus or minus 0.5 log units results in fluid temperatures of 410 °C and 570 °C, respectively. However, the ubiquitous occurrence of epidote associated with graphite in

Comment [D1]: 'its' as used here would refer to graphite, but I think epidote crystallization is meant.

the mineralized bodies points to a fO_2 at the FMQ buffer conditions and, therefore, to a temperature close to 500 ºC.

STRUCTURAL FEATURES OF GRAPHITE

The structural characterization of graphite from the Borrowdale deposit has been carried out by means of X-ray diffraction (XRD) and Raman spectroscopy (for details on analytical conditions, see Data Repository). XRD of graphite is generally used to obtain bulk information on the order of the structural arrangement along the stacking direction (c-axis) of the carbon layers. On the other hand, Raman spectroscopy records changes in crystallinity as manifested in the in-plane crystallite size (L_a), and it is a suitable analytical technique to get information on the structural homogeneity/heterogeneity of a given sample at the micrometric scale.

The XRD patterns of all the samples show sharp and symmetrical (00l) peaks, as well as (hkl) reflections of smaller intensity corresponding to fully crystalline hexagonal graphite. The average (002) spacing is 3.351 Å, and the average crystallite size along the stacking direction (L_c), calculated according to Wada et al. (1994) is 1110 Å (Table 1).

First-order Raman spectra of the studied graphite show a sharp peak at ≈1580 cm^{-1} (G band) indicative of high degree of atomic ordering, and weak or absent disorder bands at ≈1350 cm^{-1} and 1620 cm^{-1} (D1 and D2 bands, Fig. 1a). The average intensity and area ratios for the disorder to order bands (R1 = D1/G peak intensity ratio, and R2 = D1/(G+D1+D2) peak area ratio) of laminar, cryptocrystalline, and spherulitic graphite range from 0.07 to 0.09 for R1, and from 0.05 to 0.12 for R2 (Table 1). Thus, independently of the morphology of graphite, the average crystallite size L_a is in excess of 1000 Å, according to the estimation of Wopenka and Pasteris (1993). No significant

changes were observed in the second-order Raman region of graphite, all the spectra showing a well-defined shoulder at ≈2685 cm^{-1} on the S-peak. Thus, the features of the first- and second-order Raman spectra are indicative of a high degree of crystalline perfection along the basal plane of the graphite structure and also of the attainment of the triperiodic ABAB stacking (Lespade et al., 1982).

DISCUSSION

Field, petrographic, crystallographic and fluid inclusion data indicate that graphite in the Borrowdale deposit precipitated along with chlorite, epidote, quartz and albite from carbon-bearing fluids at ~500 ºC during the stage of propylitic alteration of the volcanic host rocks. This represents the first report of a deposit of highly crystalline graphite precipitated from moderate-temperature fluids.

As previously mentioned, poorly ordered, low-crystalline graphite has been observed in a wide variety of metamorphic terranes. Graphitization involves the progressive solid-state transformation of carbonaceous matter with increasing crystallinity as metamorphism proceeds. The array of carbon atoms in the graphitizable aromatic molecules of the carbonaceous matter influences the sixfold arrangement of carbon atoms within the layers of the graphite structure. That is, the original array of carbon atoms in the carbonaceous matter acts as a template during the graphitization process. Thus, graphite with low crystallinity formed under low-grade metamorphism reflects the original disordered pattern of carbon compounds within the organic matter (short continuity of the aromatic skeleton along both the in-plane directions and the stacking direction). As shown in Figure 1b, under the same analytical conditions, metamorphic graphite formed at equivalent temperatures (i.e., greenschist to epidote-

amphibolite facies) distinctively shows lower crystallinity (R1 ratio around 0.50, and average R2 close to 0.3; Beyssac et al., 2002) than that estimated in this study of the Borrowdale deposit. Therefore, firstly it may be concluded that the high crystallinity of the graphite from the Borrowdale deposit should be attributed to the different mechanism of formation of fluid-deposited graphite compared with metamorphic graphite.

However, the formation of highly crystalline graphite from low- to moderate-temperature fluids is in contrast with experimental studies which suggest that temperatures required to produce highly crystalline graphite by fluid precipitation should be higher than those operating during metamorphism of organic matter (Pasteris and Chou, 1998). Fluid-deposited graphite results from the nucleation and growth from a carbon-bearing fluid and kinetics might therefore affect the precipitation conditions and the physical properties of fluid-deposited graphite (Luque et al., 1998). Since both nucleation and growth require high activation energy (Ziegenbein and Johannes, 1980), this could be one of the reasons why highly crystalline fluid-deposited graphite is restricted mostly to high-temperature environments (Luque and Rodas, 1999; Pasteris, 1999). In addition, precipitation of graphite from low- to moderate-temperature fluids is hindered by the high solubility of carbon in such C-O-H fluids (Pasteris, 1999). Thus, compared with high-temperature, high-pressure C-O-H fluids, low-pressure, lower temperature fluids demand a very high initial concentration of carbon for graphite to be precipitated.

The data presented herein indicate that suitable conditions for the precipitation of highly crystalline graphite at moderate temperatures occurred at the Borrowdale deposit. However, experimentally re-equilibrated carbonic fluid inclusions at high temperature

Publisher: GSA
Journal: GEOL: Geology
Article ID: G25284

failed to precipitate fully crystalline graphite even at temperatures of 1400 ºC (Pasteris and Wanamaker, 1988; Pasteris and Chou, 1998). It has been shown (Ziegenbein and Johannes, 1990) that in the C-O-H system the stability field for fully crystalline graphite+fluid is larger than that for poorly ordered graphite at lower temperature (400 ºC; Fig. 2). This suggests that ordered graphite might be stabilized more readily than disordered graphite. Thus, considering that structurally disordered graphite is the phase that firstly precipitates in many experiments, Luque et al. (1998) concluded that disordered graphite is probably easier to nucleate at low temperature than is highly crystalline graphite, up to a (unknown) temperature threshold. Above this temperature, the larger size of the stability field for ordered graphite becomes the controlling factor. The results presented in this paper place the lowermost temperature limit for the precipitation of fully ordered graphite in any known volumetrically large fluid-deposited graphite occurrence.

As summarized by Luque et al. (1998) the mechanisms leading to graphite saturation in carbon-bearing fluids comprise both isochemical changes (e.g., the field of graphite+fluid is enlarged with decreasing temperature) and/or changes in the composition of the system (e.g. removal of water from the system increases the relative carbon content in the fluid, thus allowing entry into the graphite+fluid field). Temperature has been regarded as the major factor controlling the formation of fluid-deposited graphite deposits worldwide (Luque et al., 1998; Pasteris, 1999). Graphite precipitation in the Borrowdale deposit occurred as the result of the rapid cooling of the fluid as it migrated upwards along the fracture system, as evidenced by the structure of the ore bodies (pipe-like breccias) which indicates a catastrophic mineralizing event. In

addition, as previously discussed, concomitant hydration reactions involved in the propylitic alteration of the host rocks also played a role in graphite precipitation.

The final point to be addressed refers to the high carbon contents required by low- and moderate-temperature fluids to attain saturation (Pasteris, 1999). High carbon concentration in the fluids from which the Borrowdale graphite deposit was formed can be inferred on the basis of some of the graphite morphologies recognized in polished sections and are supported by fluid inclusion data. In particular, cryptocrystalline graphite and spherulitic morphologies suggest high carbon supersaturation in the fluids. These morphologies are consistent with high nucleation rates and rapid crystal growth from a large number of crystalline nuclei (Sunagawa, 1987). Moreover, the formation of cryptocrystalline and spherulitic graphite implies a mechanism of heterogeneous nucleation, that is, graphite nucleation occurs over a pre-existing substrate (mainly silicate grains). It is well known (see Sear, 2006, and references therein) that such a mechanism reduces considerably the energy barrier for nucleation with respect to the direct crystallization from an initially homogeneous fluid (homogeneous nucleation).

The results presented in this paper demonstrate that under appropriate P-T-X conditions highly crystalline graphite can precipitate at moderate temperature (~500 ºC) from fluids containing CO_2 and CH_4. This could have implications for the industrial synthesis of graphite that is currently obtained from carbonaceous precursors at much higher temperatures (>2000 ºC; Chang, 2002).

ACKNOWLEDGMENTS

The authors thank J.D. Pasteris, H. Wada and M. Satish-Kumar for constructive criticisms and helpful comments that greatly improved this paper. This work is a

contribution from project CGL2006-00835 of the Spanish Ministry of Education and Science (MEC). David Millward publishes with the permission of the Executive Director, British Geological Survey (N.E.R.C.). This study was partly funded by INSU DyETI and ANR JC (GeoCarbons project) to Olivier Beyssac.

REFERENCES CITED

Bakker, R.J., 1997, CLATHRATES: computer programs to calculate fluid inclusion V–X properties using clathrate melting temperatures: Computers & Geosciences, v. 23, no. 1, p. 1–18, doi: 10.1016/S0098-3004(96)00073-8.

Bakker, R.J., and Brown, P.E., 2003, Computer Modelling in Fluid Inclusion Research, *in* Samson, I., Anderson, A., and Marshall, D., eds., Fluid Inclusions: Analysis and Interpretation. Mineralogical Association of Canada, Short Course series, v. 32, p. 175–212.

Beyssac, O., Goffé, B., Chopin, C., and Rouzaud, J.-N., 2002, Raman spectra of carbonaceous material in metasediments: a new geothermometer: Journal of Metamorphic Geology, v. 20, p. 859–871, doi: 10.1046/j.1525-1314.2002.00408.x.

Beyssac, O., Simoes, M., Avouac, J.P., Farley, K.A., Chen, Y.-G., Chan, Y.-C., and Goffe, B., 2007, Late Cenozoic metamorphic evolution and exhumation of Taiwan: Tectonics, v. 26, p. TC6001, doi: 10.1029/2006TC002064.

Cesare, B., 1995, Graphite precipitation in C-O-H fluid inclusions: closed system compositional and density changes, and thermobarometric implications: Contributions to Mineralogy and Petrology, v. 122, p. 25–33, doi: 10.1007/s004100050110.

Chang, L.L.Y., 2002, Industrial Mineralogy. Materials, Processes, and Uses. Prentice Hall, New Jersey. 472 pp.

Duan, Z., Møller, N., and Weare, J.H., 1992a, An equation of state for the CH_4-CO_2-H_2O system: I. Pure systems from 0 to 1000 ºC and 0 to 8000 bar: Geochimica et Cosmochimica Acta, v. 56, p. 2605–2617, doi: 10.1016/0016-7037(92)90347-L.

Duan, Z., Møller, N., and Weare, J.H., 1992b, An equation of state for the CH_4-CO_2-H_2O system: II. Mixtures from 50 to 1000 ºC and 0 to 1000 bar: Geochimica et Cosmochimica Acta, v. 56, p. 2619–2631, doi: 10.1016/0016-7037(92)90348-M.

Duke, E.F., and Rumble, D., 1986, Textural and isotopic variations in graphite from plutonic rocks, South-Central New Hampshire. Contributions to Mineralogy and Petrology, v. 93, p. 409-419.

Frost, B.R., 1979, Mineral equilibria involving mixed-volatiles in a C-O-H fluid phase. The stabilities of graphite and siderite: American Journal of Science, v. 279, p. 1033–1059.

Holland, T.J.B., and Powell, R., 1998, An internally consistent thermodynamic data set for phases of petrological interest: Journal of Metamorphic Geology, v. 16, p. 309–343, doi: 10.1111/j.1525-1314.1998.00140.x.

Landis, C.A., 1971, Graphitization of dispersed carbonaceous material in metamorphic rocks: Contributions to Mineralogy and Petrology, v. 30, p. 34–45, doi: 10.1007/BF00373366.

Lespade, P., Al-Jishi, R., and Dresselhaus, M.S., 1982, Model for Raman scattering from incompletely graphitized carbons: Carbon, v. 20, p. 427–431, doi: 10.1016/0008-6223(82)90043-4.

Liou, J.G., 1993, Stabilities of natural epidotes, *in* V. Hock and F. Koller, eds, Proceedings of the 125 Jahre Kappenwand Symposium, p. 7–16.

Luque, F.J., Pasteris, J.D., Wopenka, B., Rodas, M., and Barrenechea, J.F., 1998, Natural fluid-deposited graphite: mineralogical characteristics and mechanisms of formation: American Journal of Science, v. 298, p. 471–498.

Luque, F.J., and Rodas, M., 1999, Constraints on graphite crystallinity in some Spanish fluid-deposited occurrences from different geologic settings: Mineralium Deposita, v. 34, p. 215–219, doi: 10.1007/s001260050198.

Mastalerz, M., Bustin, R.M., and Sinclair, A.J., 1995, Carbon-rich material in the Erickson hydrothermal system, northern British Columbia, Canada: Origin and formation mechanisms: Economic Geology and the Bulletin of the Society of Economic Geologists, v. 90, p. 938–947.

Millward, D., 2004, The Caradoc volcanoes of the English Lake District: Proceedings of the Yorkshire Geological Society, v. 55, p. 73–105.

Nishimura, Y., Coombs, D.S., Landis, C.A., and Itaya, T., 2000, Continuous metamorphic gradient documented by graphitization and K-Ar age, southeast Otago, New Zealand: The American Mineralogist, v. 85, p. 1625–1636.

Ohmoto, H., and Kerrick, D., 1977, Devolatilization equilibria in graphitic systems: American Journal of Science, v. 277, p. 1013–1044.

Pasteris, J.D. (1999) Causes of the uniformly high crystallinity of graphite in large epigenetic deposits. Journal of Metamorphic Geology, v. 17, p. 779-787, doi: 10.1046/j.1525-1314.1999.00231.x.

Pasteris, J.D., and Chou, I.M., 1998, Fluid-deposited graphitic inclusions in quartz: Comparison between KTB (German continental deep-drilling) core samples and

artificially re-equilibrated natural inclusions: Geochimica et Cosmochimica Acta, v. 62, p. 109–122, doi: 10.1016/S0016-7037(97)00322-0.

Pasteris, J.D., and Wanamaker, B.J., 1988, Laser Raman microprobe analysis of experimentally re-equilibrated fluid inclusions in olivine: Some implications for mantle fluids: The American Mineralogist, v. 73, p. 1074–1088.

Satish-Kumar, M., 2005, Graphite-bearing CO_2-fluid inclusions in granulites: Insights on graphite precipitation and carbon isotope evolution. Geochimica et Cosmochimica Acta, v. 69, p. 3841–3856, doi: 10.1016/j.gca.2005.02.007.

Sear, R.P., 2006, Heterogeneous and homogeneous nucleation compared: rapid nucleation on microscopic impurities: The Journal of Physical Chemistry B, v. 110, p. 4985–4989, doi: 10.1021/jp056377e.

Shi, P., and Saxena, S.K., 1992, Thermodynamic modelling of the C-O-H-S fluid system: The American Mineralogist, v. 77, p. 1038–1049.

Sunagawa, I., 1987, Morphology of Minerals, *in* Sunagawa, I., ed., Morphology of Crystals, Part B. Terra Scientific, Tokyo. p. 509–587.

Strens, R.G.J., 1965, The graphite deposit of Seathwaite in Borrowdale, Cumberland: Geological Magazine, v. 102, p. 393–406.

Wada, H., Tomita, T., Matsuura, K., Iuchi, K., Ito, M., and Morikiyo, T., 1994, Graphitization of carbonaceous matter during metamorphism with references to carbonate and pelitic rocks of contact and regional metamorphisms, Japan: Contributions to Mineralogy and Petrology, v. 118, p. 217–228, doi: 10.1007/BF00306643.

Ward, J.C., 1876, The geology of the northern part of the English Lake District. Memoir of the Geological Survey of Great Britain. Quarter Sheet 101SE (England & Wales Sheet 29, Keswick).

Wopenka, B., and Pasteris, J.D., 1993, Structural characterization of kerogens to granulite-facies graphite: Applicability of Raman microprobe spectroscopy: The American Mineralogist, v. 78, p. 533–557.

Ziegenbein, D., and Johannes, W., 1980, Graphite in C-H-O fluids: An unsuitable compound to buffer fluid composition at temperatures up to 700 °C: Neues Jahrbuch fur Mineralogie-Monatshefte, v. 7, p. 289–305.

Ziegenbein, D., and Johannes, W., 1990, Graphite-Fluid-Wechselwirkungen: Einfluss der Graphitkristallinität, *in* Emmermann, R., and Giese, P., eds, Kontinentales Tiefbohrprogramm der Bundesrepublik Deutschland, Report 90–4: Hannover, Germany, Niedersächsisches Landesamt für Bodenforschung, p. 559.

FIGURE CAPTIONS

Figure 1. A) Typical first-order Raman spectrum of laminar graphite from the Borrowdale deposit. Note the weak intensity of the D1 band at ~1355 cm^{-1} compared with the sharp and symmetrical G band at ~1580 cm^{-1}. B) First-order Raman spectrum of metamorphic graphite from Taiwan formed at 490 ºC (for details see Beyssac et al., 2007).

Figure 2. The C-O-H system at 400 ºC and 2 kbar showing the stability fields for fully ordered graphite (dotted curve) and disordered graphite (continuous line). After Ziegenbein and Johannes (1980). The area labeled BF represents the fluid compositions for the Borrowdale graphite deposit calculated from selected fluid inclusions.

Publisher: GSA
Journal: GEOL: Geology
Article ID: G25284

[1]GSA Data Repository item 2008xxx, xxxxxxxx, is available online at www.geosociety.org/pubs/ft2008.htm, or on request from editing@geosociety.org or Documents Secretary, GSA, P.O. Box 9140, Boulder, CO 80301, USA.

Publisher: GSA
Journal: GEOL: Geology
Article ID: G25284

TABLE 1. AVERAGE X-RAY DIFFRACTION AND RAMAN DATA OF GRAPHITE FROM THE BORROWDALE DEPOSIT

XRD				Raman						
n	**d_{002} (Å)**	**FWHM (°2θ)**	**Lc (Å)**	**Morphology**	**n**	**D1 position**	**G position**	**FWHM**	**R1**	**R2**
10	3.351 (0.005)*	0.311 (0.038)	1110 (130)	Laminar	21	1350.34 (2.74)	1580.75 (1.30)	20.54 (2.76)	0.09 (0.09)	0.12 (0.09)
				Cryptocrystalline	24	1354.87 (2.84)	1581.38 (1.75)	25.15 (3.57)	0.09 (0.03)	0.05 (0.08)
				Spherulitic	15	1355.88 (3.18)	1581.97 (0.92)	19.93 (1.51)	0.07 (0.07)	0.06 (0.09)

n = number of analyses.
FWHM = full width at medium height.
* Standard deviation.

Analytical techniques

The structural characterization of graphite from the Borrowdale deposit has been carried out by means of X-ray diffraction (XRD) and Raman spectroscopy. For the XRD study, after grinding and homogenization to <53 μm, ten samples of randomly orientated powders of graphite were run in a Siemens D-500 diffractometer, using Cu-Kα radiation at 30 kV and 40 mA, a step size of 0.03 (º2θ), a slit system of 1º-1º-1º-0.15º, and time per step of 1 s (scan rate of 1.8º 2θ/min). Each sample was run at least twice using silicon as the internal standard. Measurements on the XRD patterns were done using the Diffrac Plus EVA 10.0 software.

Raman spectra were collected with the Renishaw INVIA equipment at the Ecole Normale Superieure (Paris, France) on polished thin sections used for the petrographic study. A total of 60 measurements were obtained focusing the laser beam on graphite located beneath the surface of adjacent transparent minerals (usually quartz, chlorite, and epidote) to avoid the effect of polishing at the surface of the thin section which may alter the graphite structure (Pasteris, 1989; Beyssac et al., 2003). The 514.5 nm wavelength of a 20 mW Spectra Physics Argon laser focused through a 100x objective (N.A.=0.90) was used for the analyses. Under these conditions the spatial resolution is ~1 μm and the spectral resolution is close to 1 cm^{-1}. Laser power on the sample surface was reduced to 2 mW to avoid radiation damage to the graphite. Raman analysis of graphite also might be affected by polarization effects between the incident laser electromagnetic field and the structure of graphite, and this might virtually enhance the defect bands especially for measurement on the graphite edge planes. These effects are rather weak with a 514.5 nm wavelength (Tan et al., 2004), and to further attenuate them we used a ¼ wavelength plate before the microscope which yields a circular polarization of the laser. The Raman parameters (peak position, band intensity, and band area) were determined with the computer program PeakFit 3.0 using a Voigt function.

The microthermometric study of the fluid inclusions was carried out using a Linkam THMSG 600 heating and freezing stage at the Department of Crystallography and Mineralogy, Universidad Complutense, Madrid. Raman analysis of the volatile fraction was also performed at the Ecole Normale Superieure under the same analytical conditions given above, but the laser power in this case was 50 mW. Bulk composition, density and molar volume of the inclusions were calculated with the computer programs

DENSITY, ICE and BULK, versions 12/02 (Bakker and Brown, 2003) using the Duan et al. (1992a,b) equation of state and considering NaCl as the only salt in solution.

Fluid inclusions data

Fluid inclusions were studied in quartz fragments hosted by the graphite nodules-bearing pipes (Figure DR1). The angular shape of these fragments and their internal grainy texture indicate that the quartz was brecciated, pulled up from its original location and transported upwards within subvertical structures favoured by a fluid-rich regime that eventually resulted in the precipitation of huge amounts of graphite. These fluids were recorded as secondary fluid inclusions in the quartz xenoliths. Three types of secondary fluid inclusions have been recognized, based upon appearance at room temperature and microthermometric behaviour:

Type V. Two-phase vapour-rich inclusions (Vv/Vt = 60-90%), made up by H_2O-CO_2- CH_4. These inclusions are very abundant and occur along trails within the clear cores of the quartz grains. Raman data of the volatile fraction indicate mixtures of CO_2-CH_4, with XCO_2 between 0.6-0.75. The average bulk composition (mol fraction) of these inclusions is 0.65 H_2O, 0.24 CO_2, 0.11 CH_4 and 1.4 wt% NaCl, with a $XCO_2/(XCO_2+XCH_4)$ ratio of 0.69 and an average molar volume of 40 $cm^3.mol^{-1}$. Total homogenization of the inclusions ranges 295-340 ºC (into vapour) and 328-350 ºC (critical behaviour) indicating that the fluid would be a vapour-like supercritical phase at the trapping conditions. Complete microthermometric and compositional data of selected type V inclusions can be found in Table DR1.

Type L1. Two-phase liquid-rich H_2O-CO_2- CH_4-bearing inclusions (Vv/Vt = 25-40%). These inclusions are very scarce and occur spatially associated with type V inclusions. Raman analysis indicate XCO_2 between 0.03-0.28 in most L1 inclusions (n=6) and only two specimens with XCO_2=0.6-0.62. Bulk composition (mol fraction), calculated only in one inclusion due to the difficulty of measuring clathrate melting, is estimated to be 0.916 H_2O, 0.018 CO_2, 0.022 CH_4 and 0.044 NaCl (7.2 wt% NaCl), with a $XCO_2/(XCO_2+XCH_4)$ ratio of 0.45 and a molar volume of 25 $cm^3.mol^{-1}$. Total homogenization occurs between 279 and 378 ºC, in a range which is similar to homogenization temperatures for type V inclusions. However, whereas type V homogenizes either by bubble expansion or show critical behaviour, L1 inclusions always homogenize into liquid.

Type L2. Two-phase liquid-rich inclusions (Vv/Vt < 10%). They are very abundant and occur along trails that occasionally cross-cut quartz grain boundaries, thus

indicating that the inclusions are secondary in origin and postdate the type V and L1 fluid circulation. They also occur in recrystallized boundaries of the quartz grains, probably as primary inclusions. CH_4 is the only carbonic species in these inclusions, with an estimated average composition of 0.93 H_2O, 0.02 CH_4 and 0.05 NaCl. Melting of ice occurs in the range -6 to -2.8 ºC and indicates salinities between 4.5 and 9.5 wt% NaCl. The total homogenization of the L2 inclusions occurs between 123 and 204 ºC, with a maximum in the interval 180-190 ºC.

These fluid inclusions assemblages have been interpreted to be the record of the evolution of the carbon-bearing fluids involved in the pipes development and the subsequent graphite deposition. In this scenario, the type V vapour-rich fluid would be the fluid circulating at the earliest stages of the process just before graphite saturation was reached. Therefore, the physicochemical parameters estimated from this fluid would indicate the initial P-T-fO_2 conditions of the graphite forming system which are the aim of this paper.

References cited

Bakker, R.J., and Brown, P.E., 2003, Computer Modelling in Fluid Inclusion Research, in Samson, I., Anderson, A., and Marshall, D., eds., Fluid Inclusions: Analysis and Interpretation. Mineralogical Association of Canada, Short Course series, v. 32, p. 175–212.

Beyssac, O., Goffé, B., Petitet, J.P., Froigneux, E., Moreau, M., and Rouzaud, J.-N., 2003, On the characterization of disordered and heterogeneous carbonaceous materials by Raman spectroscopy. Spectrochimica Acta, Part A, v. 59, p. 2267-2276.

Duan, Z., Møller, N., and Weare, J.H., 1992a, An equation of state for the CH4-CO2-H2O system: I. Pure systems from 0 to 1000 ºC and 0 to 8000 bar: Geochimica et Cosmochimica Acta, v. 56, p. 2605–2617, doi: 10.1016/0016-7037(92)90347-L.

Duan, Z., Møller, N., and Weare, J.H., 1992b, An equation of state for the CH4-CO2-H2O system: II. Mixtures from 50 to 1000 ºC and 0 to 1000 bar: Geochimica et Cosmochimica Acta, v. 56, p. 2619–2631, doi: 10.1016/0016-7037(92)90348-M.

Pasteris, J.D., 1989, In situ analysis in geological thin-sections by Laser Raman Microprobe Spectroscopy: a cautionary note. Applied Spectroscopy, v. 43, p. 567-570.

Tan, P.H., Dimovski, S., and Gogotsi Y., 2004, Raman scattering of non-planar graphite: arched edges, polyhedral crystals, whiskers and cones. Philosophical Transactions of the Royal Society of London, part A, v. 362, p. 2289-2310, doi: 10.1098/rsta.2004.1442.

TABLE DR1. MICROTHERMOMETRIC, RAMAN AND CALCULATED COMPOSITIONAL DATA OF SELECTED TYPE V INCLUSIONS FROM THE BORROWDALE DEPOSIT

	Non aqueous phase data						Bulk inclusion data						
Vv/Vt	**$TmCO_2$**	**$ThCO_2$**	**TmCl**	**XCO_2**	**XCH_4**	**Molar volume**	**XH_2O**	**XCO_2**	**XCH_4**	**Salinity**	**TH**	**Bulk molar volume**	**#XCO_2**
0.8	-58.4	+1.5 L	+14.2	0.64	0.36	75.43	0.49	0.33	0.18	3.03	294 *	46.50	0.65
0.5	-57.4	+8.9 L	+14.2	0.75	0.25	75.52	0.78	0.17	0.05	0.47	340 C	29.66	0.43
0.7	-	+3.8 L	+14.2	0.75	0.25	77.29	0.63	0.28	0.09	0.28	300 *	39.50	0.76
0.7	-	-8.1 L	+14.2	0.60	0.40	86.52	0.64	0.21	0.13	2.86	295 *	40.90	0.62
0.7	-58.7	-1.9 L	+14.4	0.67	0.33	81.78	0.64	0.245	0.11	1.36	293 *	40.21	0.69
0.7	-	+3.3 L	+14.2	0.75	0.25	76.16	0.62	0.29	0.09	0.4	318 V	39.30	0.76
0.6	-61.8	+5.1 L	+14.2	0.69	0.31	74.99	0.71	0.20	0.08	2.02	340 V	33.62	0.71
0.9	-	+4.1 L	+14.2	0.68	0.32	75.83	0.0024	0.768	0.23	-	322 V	84.26	0.77

Molar volume in $cm^3.mol^{-1}$, salinity in eq. NaCl wt%, temperature in ºC. Vv/Vt: bubble volume fraction, X: molar fraction, Tm: melting temperature, Th: partial homogenization temperature, TH: total homogenization temperature, Cl: clathrate, #XCO_2= $XCO_2/(XCO_2+XCH_4)$, * Decrepitation temperature before homogenization, C: critical homogenization, L: homogenization into liquid, V: homogenization into vapour.

Figure DR1. Hand specimen of the common graphite-quartz association from the Borrowdale deposit. Note the large angular quartz fragment (Qtz), and the intense alteration of the andesite host rock (AA). Small quartz fragments are also embedded within the graphite mass (Gph).

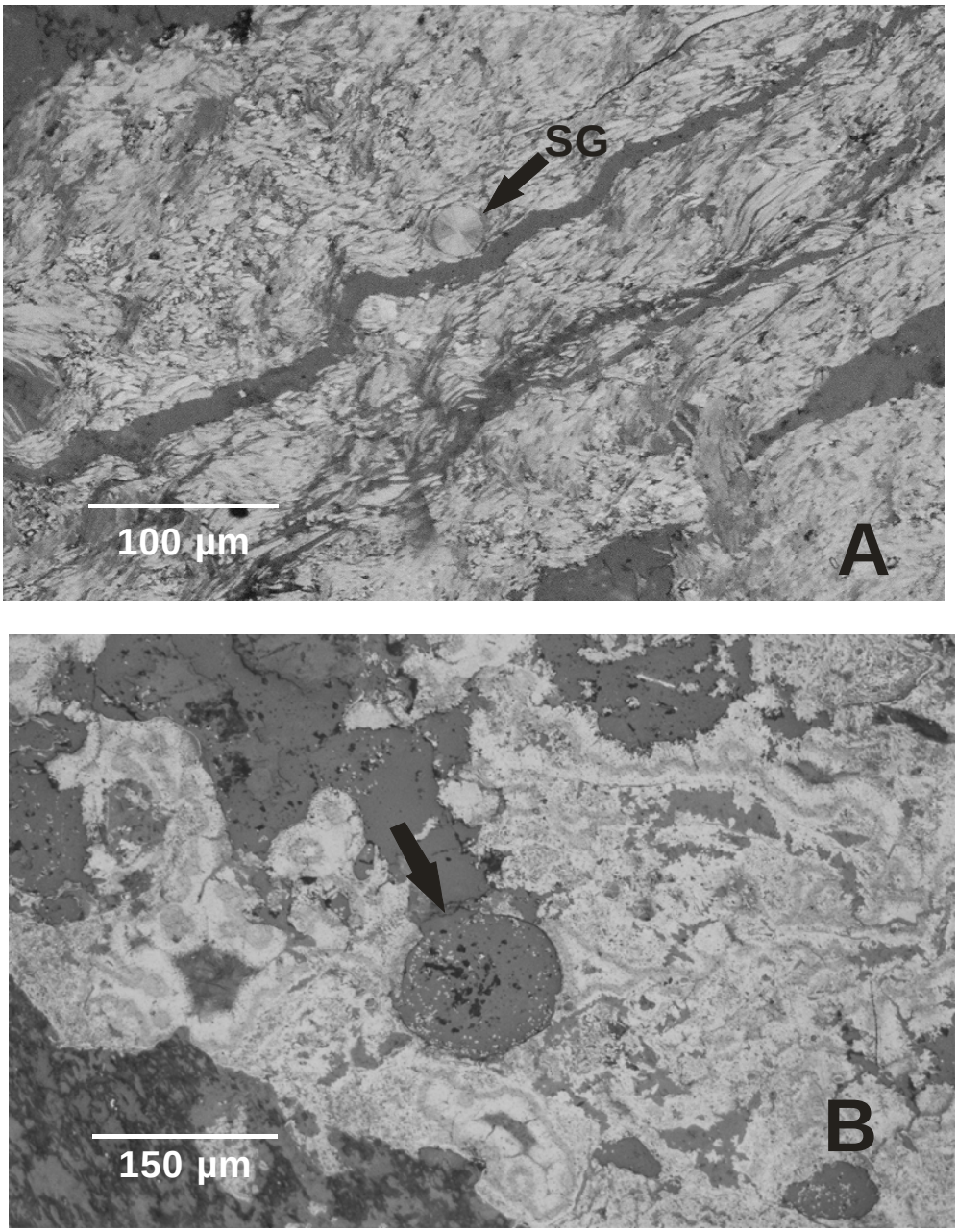

Figure DR2: Reflected light photomicrographs (one polar) of graphite morphologies from the Borrowdale deposit. A) Spherulitic graphite (SG) within flaky graphite. B) Cryptocrystalline graphite with colloform texture enclosing quartz grains. The arrow indicates a rounded quartz grain containing minute spherulites of graphite.

Figure DR3: Transmitted light photomicrograph showing radial aggregates of epidote crystals within a graphite (in black) nodule.

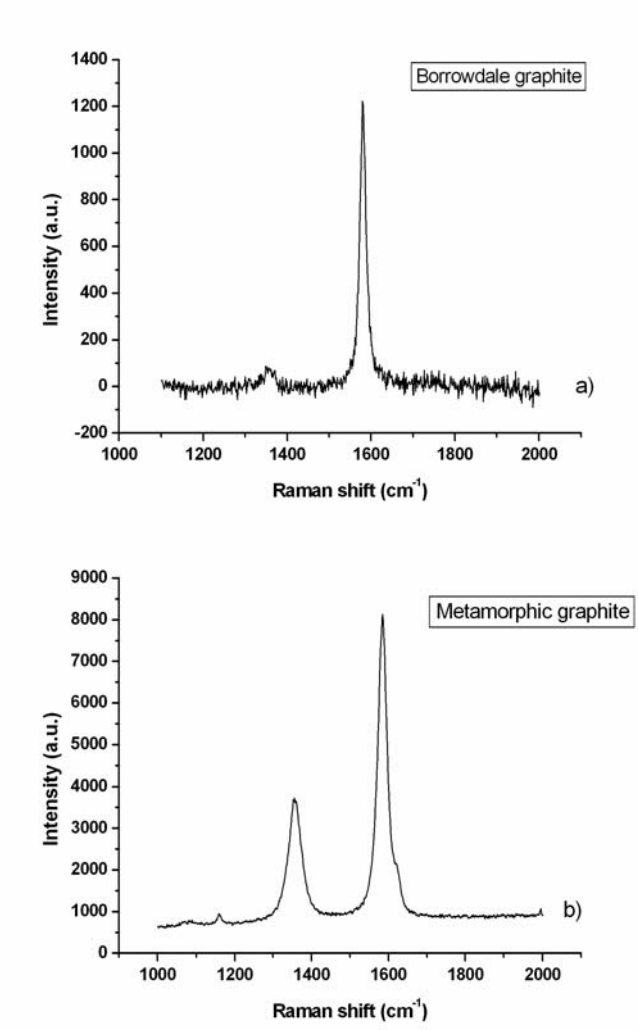
Borrowdale graphite
Intensity (a.u.)
Raman shift (cm-1)
a)
Metamorphic graphite
Intensity (a.u.)
Raman shift (cm-1)
b)

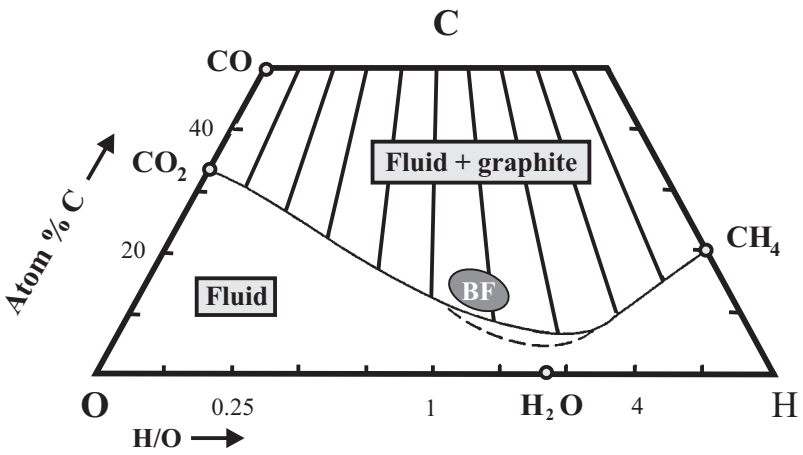
C
CO
40
CO2
Fluid + graphite
CH4
Atom % C
20
Fluid
BF
O
0.25
1
H2O
4
H
H/O